

ASSESSMENT OF LOCAL DERIVED IONOSPHERIC MODEL IN BASELINE AMBIGUITY RESOLUTION

Siti Syukriah Khamdan*¹, Tajul Ariffin Musa¹, Suhaila M. Buhari^{1,2}, Neil Ashcroft³, and Ahmad Nashriq Ferdaus³

¹Geomatic Innovation Research Group (GnG), Faculty of Built Environment and Survey, Universiti Teknologi Malaysia, Malaysia

²Department of Physics, Faculty of Science, Universiti Teknologi Malaysia, Malaysia.

⁴Regional Technical Support, Asia Sales, Leica Geosystems ASIA, Singapore.

syukriahkhamdan91@gmail.com



OUTLINE

01



INTRODUCTION

METHOD AND STUDY AREA



02

03



RESULTS AND DISCUSSION

CONCLUSION



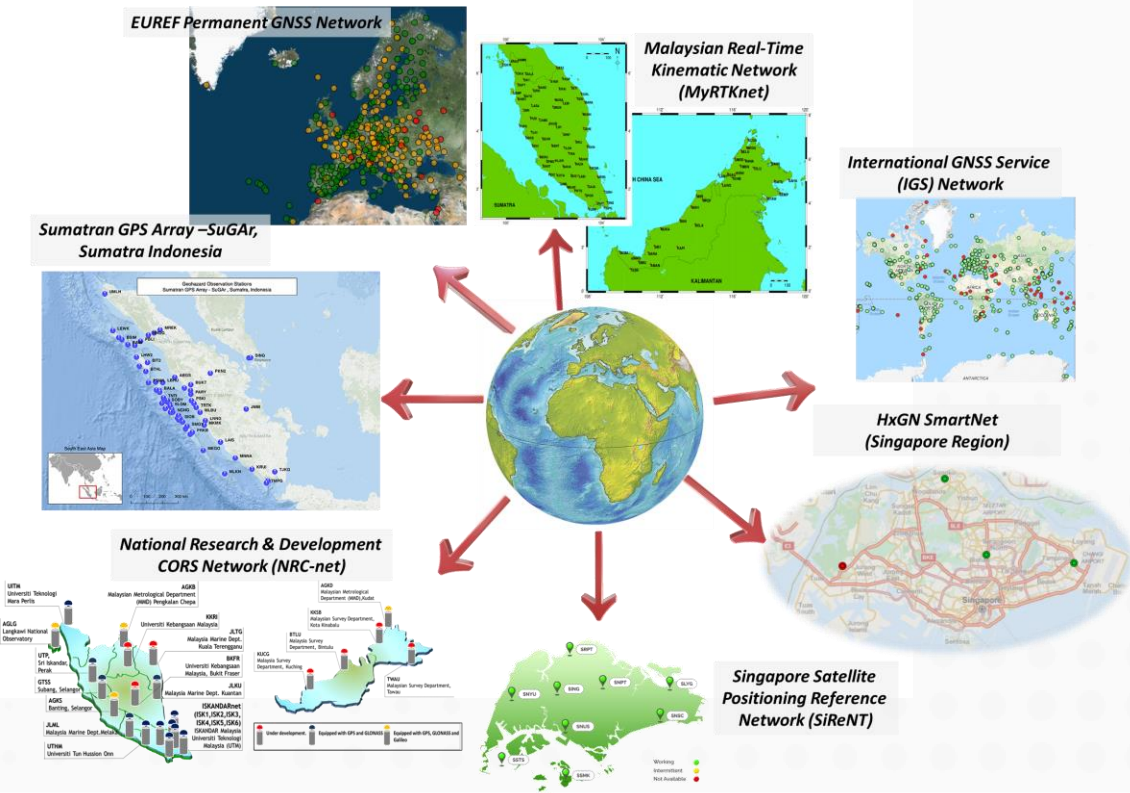
04

INTRODUCTION

- The global positioning system (GPS) signals propagate from satellite to receiver, passing through the ionosphere layer – resulting in time – degrading the accuracy of GPS positioning and navigation applications (Leong et al. 2011; Sunehra 2013; Pathy et al. 2019).
- The ionospheric conditions affect the GPS applications, especially over the equatorial region – seasonal, geomagnetic activities, solar activities, and ionospheric irregularities: equatorial electrojet (EEJ) (Yamakazi and Kosch 2015), equatorial plasma bubbles (EPB) (Sarudin et al. 2017), equatorial ionization anomaly (EIA) (Khamdan et al. 2019) , equatorial spread-F (ESF) (Zakharenkova and Cherniak 2021) and field-aligned irregularities (FAI) (Martiningrum et al. 2020).
- With this as an advantage, the GPS has been used widely as a tool for studying and monitoring the ionospheric conditions – presented in total electron content (TEC) parameters.
- In high-precision GPS positioning, the ionosphere-linear combination has been used to minimize the ionospheric delay in order to solve the ambiguity of the baseline – the ionosphere scale factor (ISF) is minimal with a value of 0.0 (Musa 2007). Meanwhile, others linear combinations need to use the ionospheric model.

GPS station at Kudat, Sabah (AGKD), under National R&D CORS Network (NRC-net) – managed by Geomatic Innovation Research Group (GnG), UTM together with Malaysian Space Agency (MySA).

GPS station at Woodland Singapore (LGT1) – managed by Leica Geosystems Singapore



Example of GPS CORS network that is available (Regional GPS Network/Global GPS Network).

INTRODUCTION

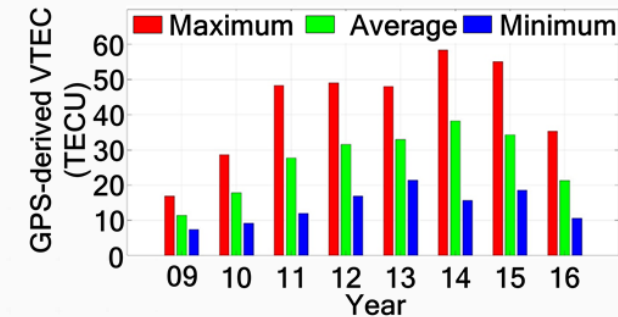
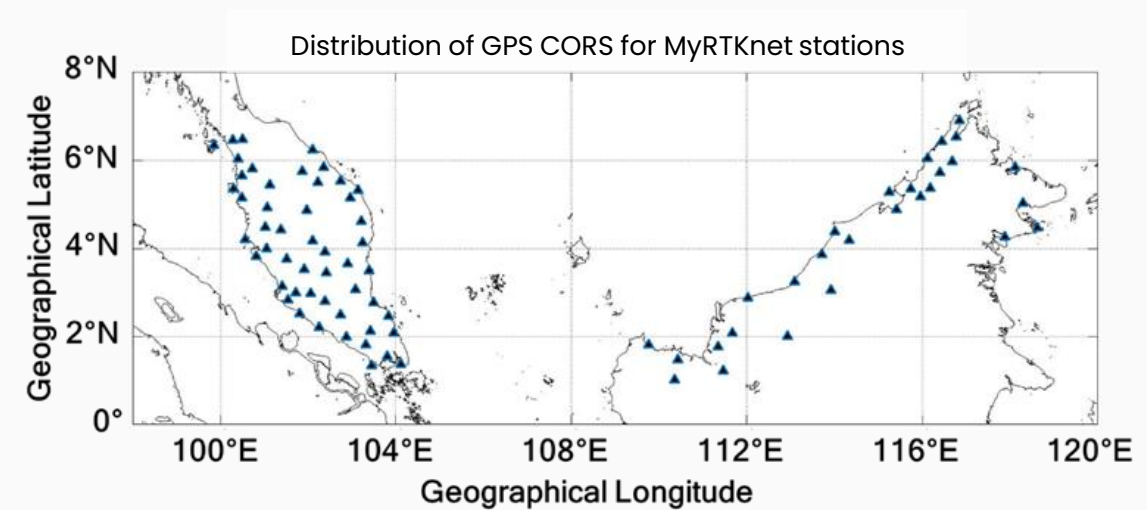
- The suitability of the ionospheric model depends on the scale of the area – global or regional/local scale.
- The Global Ionospheric Maps (GIM) has a good accuracy – 2 to 8 TECU (de Oliveira et al. 2021) – most studies directly used to solve the GPS baseline ambiguity especially for high precision processing software (Banville et al. 2014; Weilgosz et al. 2021).
- The GPS ambiguity resolution is the process of estimating the integer parameters of the GPS carrier phase observation. This process is important as it is a key to high precision relative GPS positioning especially when involved with only short observation time (Verhagen, 2015).
- Even though the implementation of the global ionospheric model improved/solved the ambiguity of the baseline (in terms of accuracy and precision), however, there are several limitations:
 - the global ionospheric model best describes the global conditions of the ionosphere (Khamdan 2018; Klimenko et al. 2018; Ren et al. 2022).
 - Different ionospheric conditions affect the ambiguity resolution differently, especially when involved with a long baseline of more than 1000 km (Hernandez-Pajares et al. 2000; Khodabandeh and Teunissen 2018).
 - Interpolation in providing the ionospheric correction that leads to the limited precision and resolution (El Manaily et al. 2018; Mengist et al. 2019).
- A precise ionospheric model is important – to mitigate the influence of the ionospheric delays on the GPS applications during occurrences of ionospheric irregularities (Jacobsen and Andalsvik 2016; Ciecko and Grunwald 2020) – causing to loss of lock GPS signals and leading to reinitialization of ambiguity (Tang et al. 2017; Damaceno et al. 2020).

INTRODUCTION

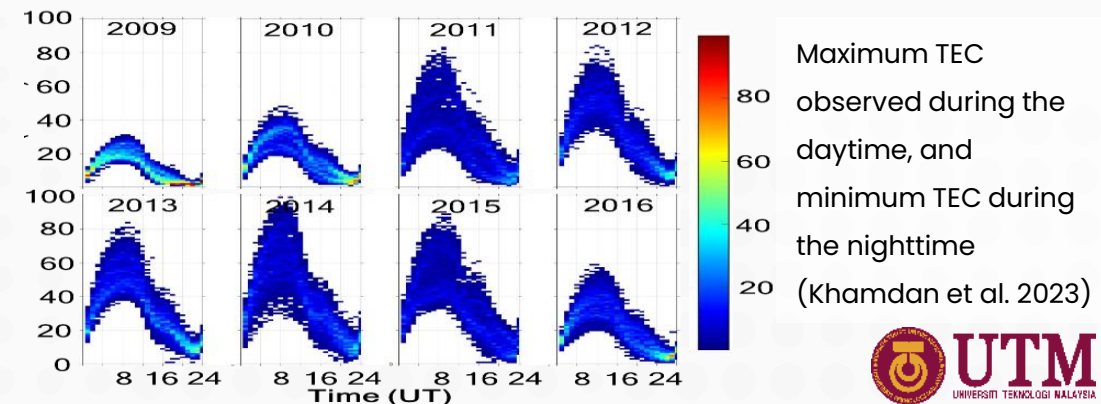
- Previously
 - Colombo et al. (2002) applied the locally derived ionospheric model generated from a tomography technique to a wide-area network RTK. They assessed the performances of the models with the length of the baseline up to hundreds of kilometers under different conditions of ionospheric activities.
 - Assiadi et al. (2014) improve the accuracy of single-epoch positioning of GPS over the California area. The result shows an improvement in coordinates up to 10 cm – 20 cm for baseline ranging between 60 to 120 km. This is one of the steps forward in developing the local ionospheric model over the area.
 - Psychas et al. (2019) investigate the performances of the RTK solutions using the ionospheric correction generated from the local network. The result demonstrates the fastest solutions (carrier phase fixed ambiguity) available with the ionospheric correction can be obtained up to 5 cm (~0.31 TECU).
 - Silva et al. (2020) investigate the performances of the local ionospheric model in solving the ambiguity of the long baseline during the weak and strong ionospheric activity, with the ambiguity percentage values up to 80.1% and 67.4%, respectively for the Brazil area.
 - Zhang et al. (2022) resolved the ambiguity of long baseline by using BDS-3 and quad-frequency ionosphere weighted model over China with a percentage ambiguity resolution up to 98% compared to the dual-frequency ionosphere free.

METHOD & STUDY AREA

- Aim: To assess the performances of the locally derived ionospheric model in solving the baseline ambiguity.
- Flow:
 - Derive the ionospheric model from local GPS CORS network (MyRTKnet) over the Malaysian region.
 - Apply the local ionospheric model into baseline processing.
 - Analyzed the performances of the local ionospheric model: percentage improvement and comparison of baseline vector with true value (AUSPOS).
- 5 baselines consist of:
 - 1 Short baseline (<100 km)
 - 1 Medium baseline (<500 km),
 - 1 Long baseline (<1000 km), and
 - 2 very long baselines (>1000 km), where 1 baseline formed outside generated region of local ionospheric model.
- The assessments are based on two case studies:
 - a. Case 1: Occurrences of ionospheric irregularities (EPB) – 5th April 2011, and
 - b. Case 2: During Geomagnetic storms – 31st Aug (G1) and 1st Sept 2019 (G2)



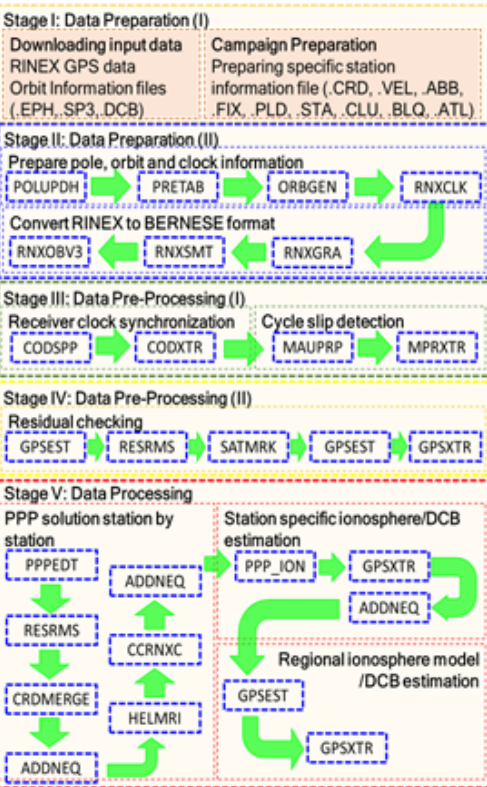
The trend of the ionospheric variations over the Malaysian region: Increased and decreased with the solar cycle (Khamdan et al. 2023)



Flow chart and processing parameters for the derivation of the local ionospheric model using Bernese Software 5.2 (Khamdan et al. 2023).

METHOD & STUDY AREA

Strategy for baseline processing during the application of the ionospheric model.



Parameter	Value
Software	Bernese Software Version 5.2
Satellite System	GPS only
Orbit and Pole	IGS precise final orbit (SP3) and Earth Orientation Parameter
Basic Observable	Carrier Phase and Smoothed Code
Elevation Cut Off Angle	5°
Sampling Interval	30 Seconds
Number of Coefficients	
Maximum degree of spherical harmonic	5
Maximum order of spherical harmonic	5
Modeling Characteristic	
Model of temporal modeling	Static
Reference frame definition	Geomagnetic
Longitude of the sun	Mean
Mapping function	Modified Single Layer Model (MSLM)
A prior height of single layer	400 km
Latitude of geomagnetic pole	79°
Longitude of geomagnetic pole	-71°
Temporal resolution	1- hour

Processing Strategy and Parameter Estimation		Description
Resolution Strategy	SIGMA using wide-lane linear combination	The SIGMA-dependent strategy used the full variance-covariance information.
	QIF using ionosphere free linear combination	The Quasi-Ionospheric-free (QIF) ambiguity resolution strategy resolve L1 and L2 ambiguities directly without using the code measurement.
Sampling Rate	30 seconds	The sampling rate of GPS data observation.
Elevation Mask	15°	The elevation mask was used to resolve the ambiguity resolution.
Ionosphere Model	Without ionospheric model	The models were used to determine the performance of the ambiguity resolution.
	Local ionospheric model	The local ionospheric model was estimated using Bernese software as described in the previous section, while the global ionospheric model was obtained from the CODE analysis center.
	Global ionospheric model	

Assessments:

- Improvement of the percentage ambiguity resolution, and
- Comparison of baseline vectors with known values (AUSPOS).

$$\Delta dX = dX_{estimated} - dX_{AUSPOS}$$

$$\Delta dY = dY_{estimated} - dY_{AUSPOS}$$

$$\Delta dZ = dZ_{estimated} - dZ_{AUSPOS}$$

Where $dX_{estimated}$, $dY_{estimated}$, and $dZ_{estimated}$ represent the estimated baseline vectors and dX_{AUSPOS} , dY_{AUSPOS} , and dZ_{AUSPOS} represent the known values of the baseline vector from AUSPOS GPS Online Processing.

The baselines processed without applying an ionospheric model serve as a benchmark to monitor the improvement in ambiguity resolution by both ionospheric models.

RESULTS

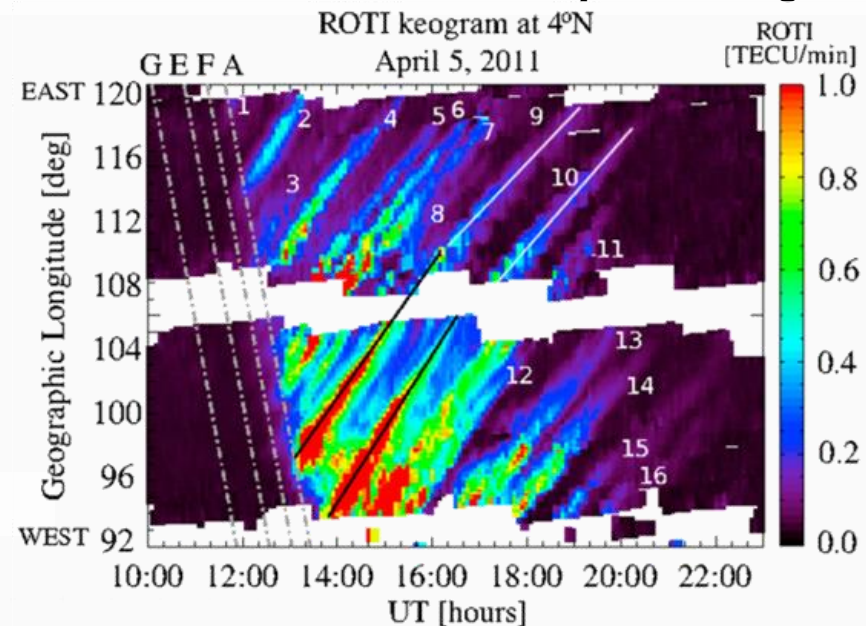
Information of the GPS CORS that are involved

Type of Baselines	GPS CORS		Baseline Name	Baseline Length (km)
Short	MERU (3.14°N, 101.41°E)	UPMS (2.99°N, 101.72°E)	MEUP	39
Medium	AYER (5.75°N, 101.86°E)	KROM (2.76°N, 103.50°E)	AYKR	377
Long	AMAN (1.12°N, 111.46°E)	BEAU (5.41°N, 115.73°E)	AMBE	659
Very Long	DATU (5.03°N, 118.29°E)	UUMK (6.46°N, 100.51°E)	DTUU	1969
	MLKN (-5.35°N, 102.28°E)	UMLH (5.05°N, 95.34°E)	MLUM	1382

Maps of the baselines that are formed and GPS CORS locations that are involved.



Case 1: Occurrences of Ionospheric Irregularities (EPB) on 5th April 2011

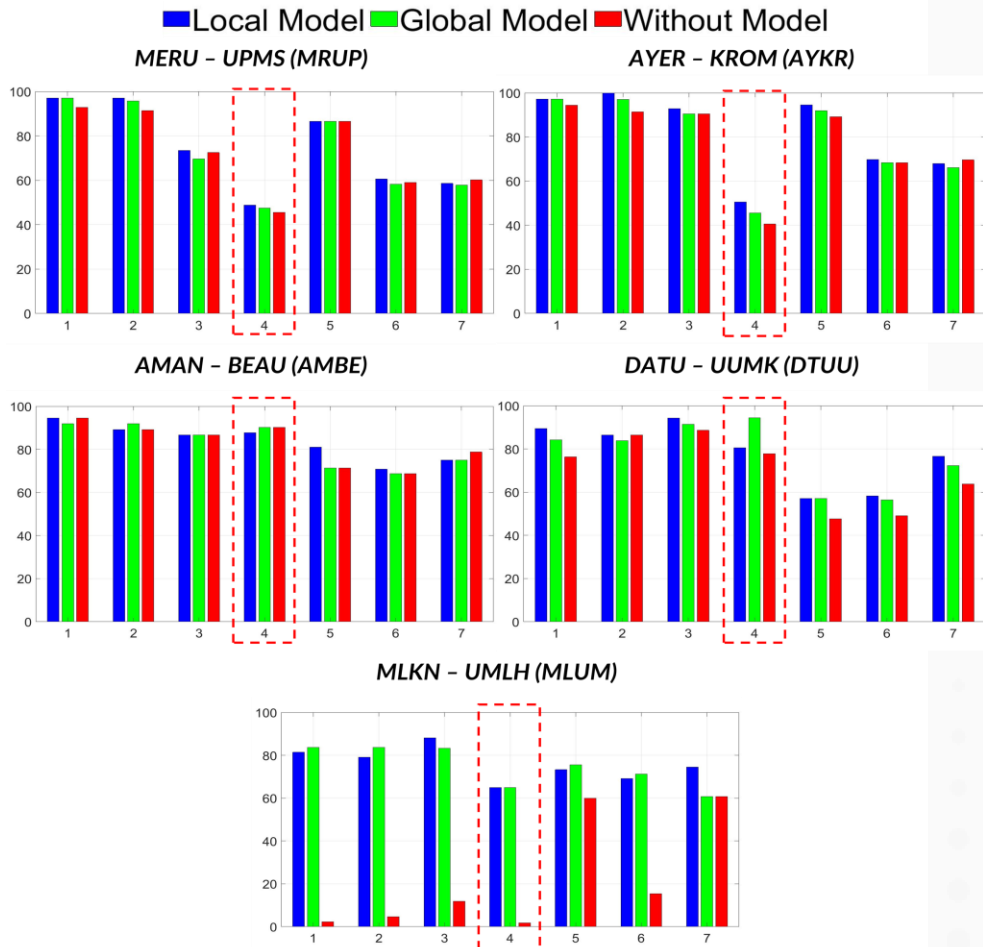


- Buhari et al. (2014) observed at least 16 striations of EPB structure on night-time 5th of April 2011 at the cross-section of 4°N over Southeast Asia.
- Based on the airglow observation, the attenuation compared to the background intensity was about 10% to 20%.

- Study period: 2nd April 2011 (DoY 092) until 8th April 2011 (DoY 098), which included the day with EPBs and three days before and after the days with EPBs.
- Since the EPBs are large-scale irregularities, constructive or destructive interference can occur when signals from GPS cross the ionospheric layer. The occurrences of EPBs can cause rapid changes in the ionosphere which can result in the loss of lock of the GPS signals and lead to a cycle slip and difficulty in resolving the ambiguity (Banville et al. 2010).

RESULTS

Case 1: Occurrences of Ionospheric Irregularities (EPB) on 5th April 2011

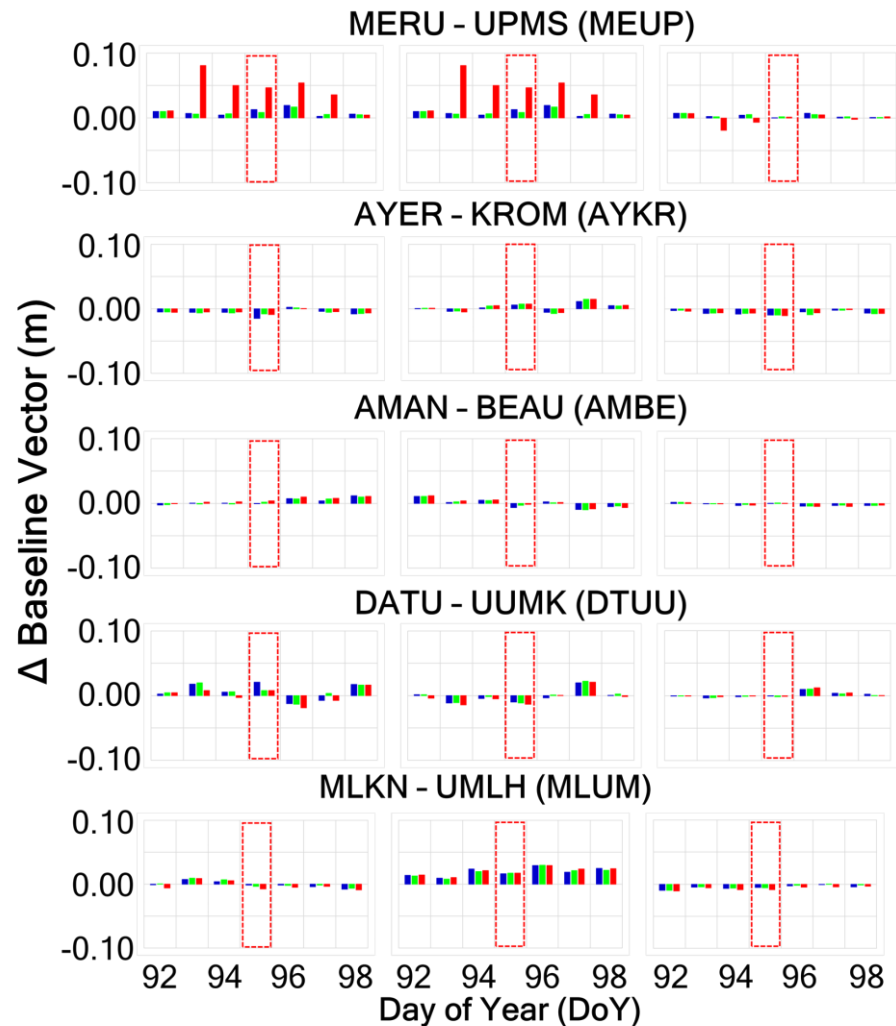


- Ambiguity Resolution:
 - Both ionospheric models improved the percentage of the ambiguity resolution for all baselines.
 - The percentage of ambiguity resolution was lower during the day with EPBs, especially for short and medium baseline, with a percentage up to 40%.
 - Since the baseline is less than 500 km long and had almost similar ionospheric conditions, this result could be due to the quality of the data (cycle slips) in the observations due to the occurrences of EPBs (Banville et al. 2014).
 - For very long baseline MLUM, both global and local show similar percentage values up to 64.9%. The ambiguity without the ionospheric model is shown at 1.8% only, which is expected as large differences in ionospheric conditions between the stations involved.

The percentage of ambiguity resolution for the GPS baselines. The dashed red box represents the day with EPB.

RESULTS

Case 1: Occurrences of Ionospheric Irregularities (EPB) on 5th April 2011

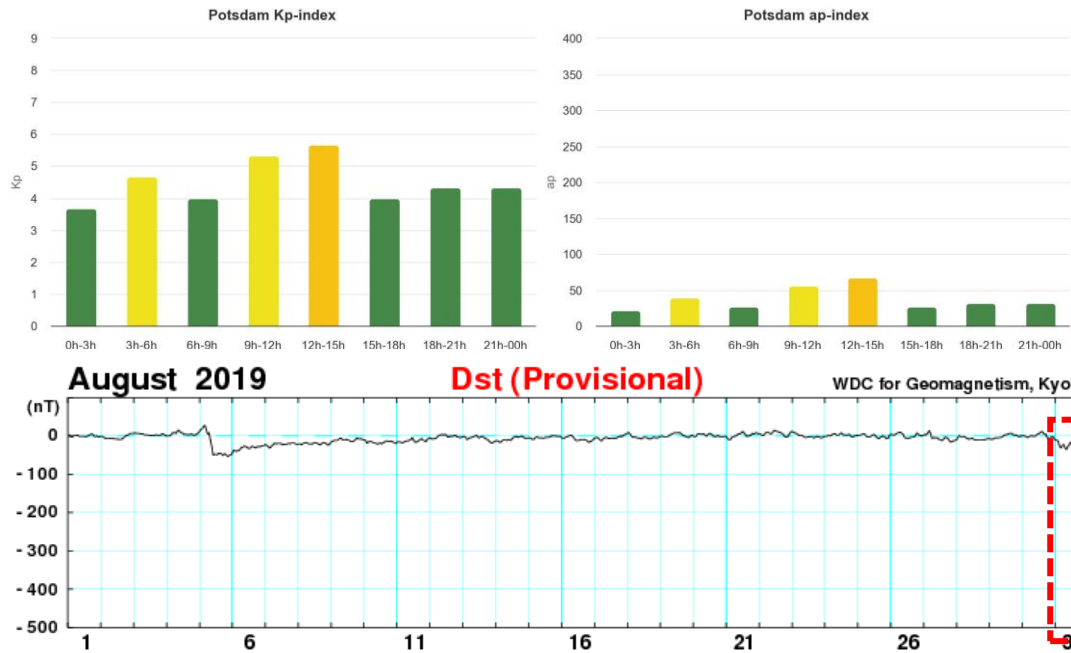


Comparison of the baseline vector. The left column represents the ΔdX , the middle column represents the ΔdY and the right column represents the ΔdZ . The red boxes highlight the day with EPBs.

- Comparison of Baseline Vector (purpose to validate and determine the processing quality of ambiguity resolution)
 - Minimal difference in baseline vectors for both models, with values within ± 2 cm for all components.
 - Even though the percentage ambiguity is small ($< 50\%$), the differences are only minimal for all baselines during the day with EPB.
 - For MLUM, large differences are observed especially for ΔdY components which may be due to the minimal percentage of the ambiguity resolutions and also contributed by the quality of the observation data itself.
 - Meanwhile, a large difference in the MEUP baseline without the ionospheric model was observed. Even though the ambiguity is high, this could be due to the frequent false ambiguity resolution (Yang et al. 2020), and lead to the degradation of the accuracy and precision of GPS positioning (Souza and Monico 2007).

RESULTS

Planetary indices on 31st August 2019 (G1) geomagnetic storm.



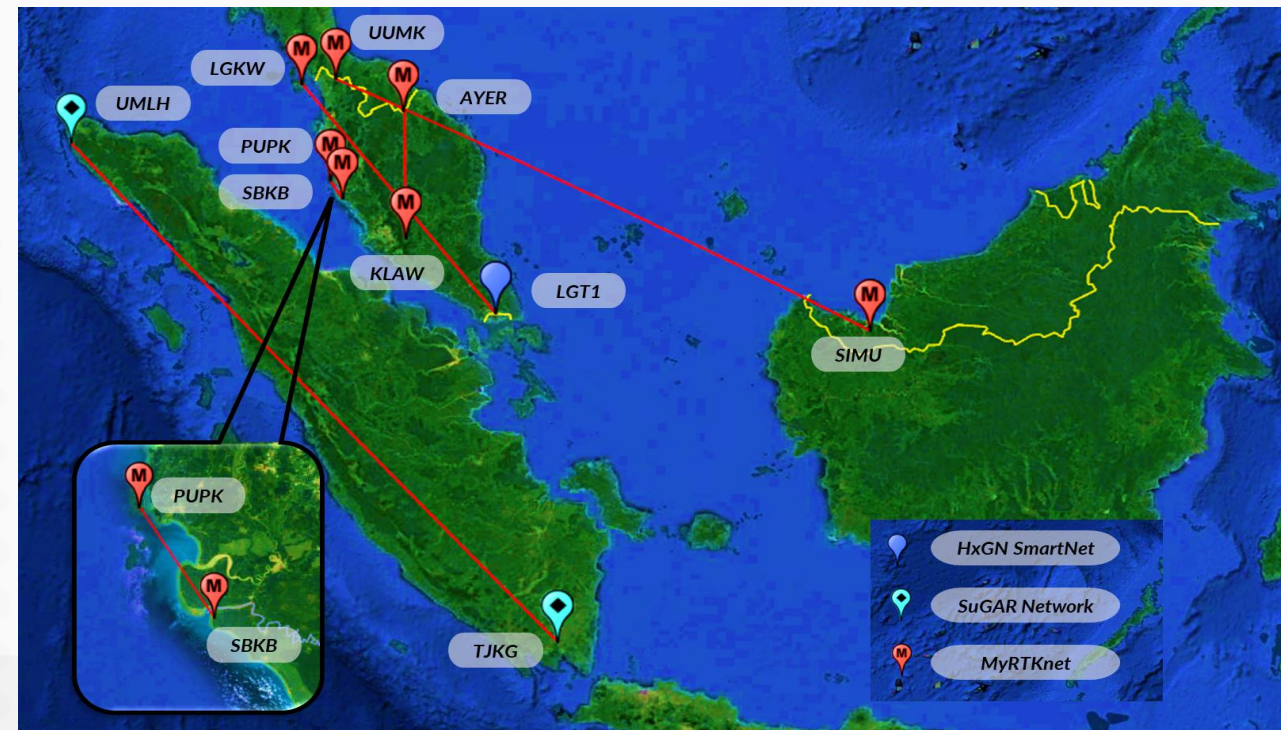
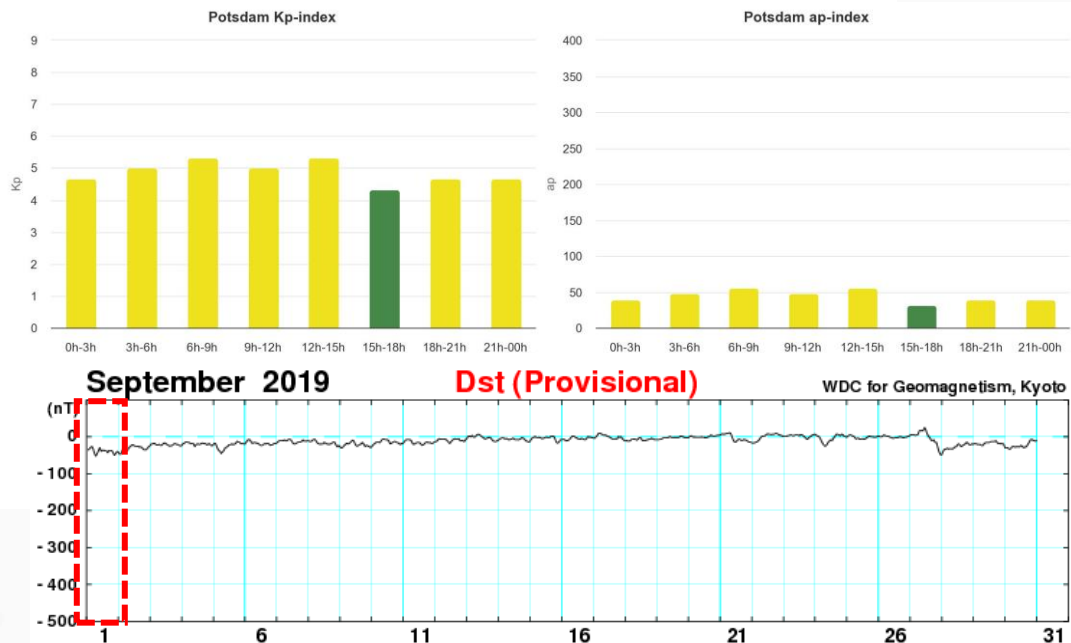
Case 2: Geomagnetic Storms on 31st August 2019 (G1) and 1st September 2019 (G2)

Type of Baselines	GPS CORS		Baseline Name	Baseline Length (km)
Short	PUPK (4.21°N, 100.56°E)	SBKB (3.81°N, 100.82°E)	PPSB	52
	AYER (5.75°N, 101.86°E)	KLAW (2.98°N, 102.06°E)	AYKW	306
Long	LGT1 (1.45°N, 103.81°E)	LGKW (6.33°N, 99.85°E)	L1LG	693
	SIMU (1.36°N, 110.79°E)	UUMK (6.46°N, 100.51°E)	S4UU	1273
Very Long	UMLH (5.05°N, 95.34°E)	TJKG (-5.24°N, 105.17°E)	UMTJ	1579

2019 (G2)

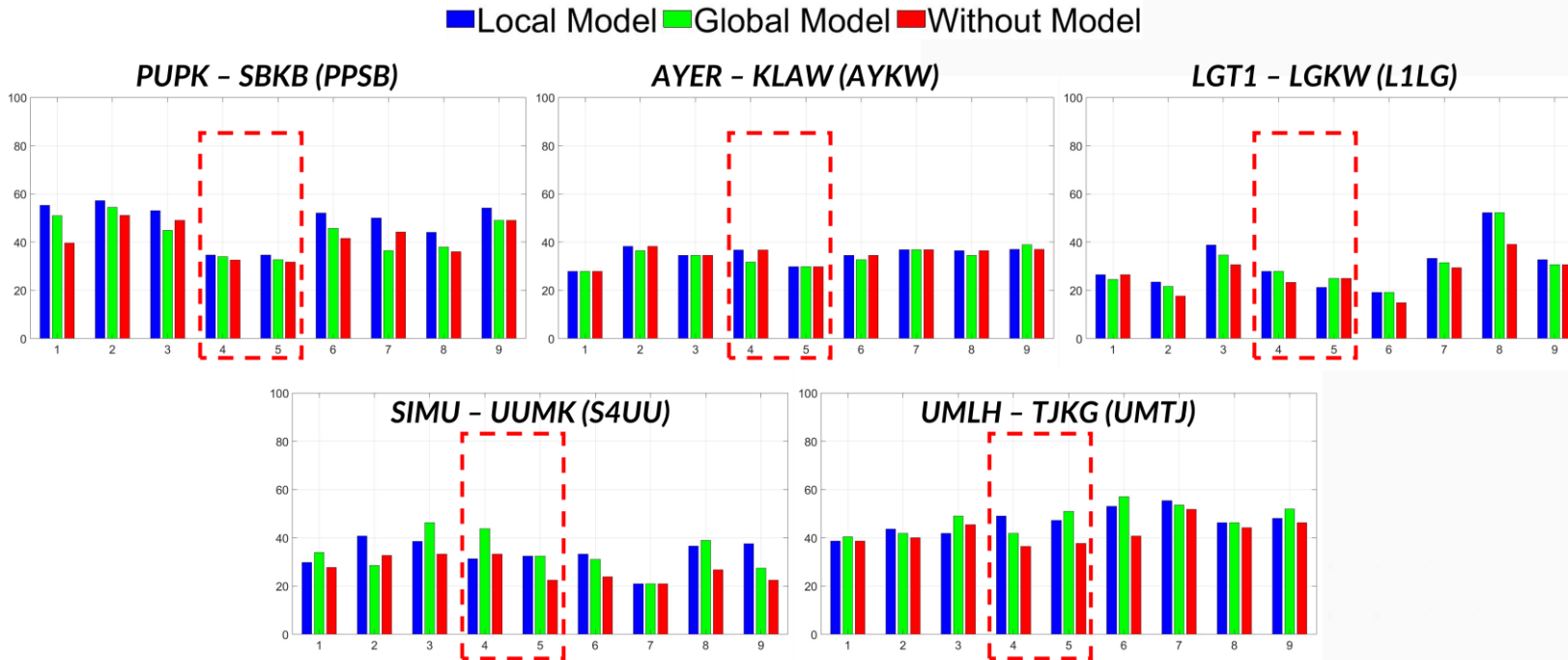
Study period: 28th August 2019 (DoY 240) until 5th September 2019 (DoY 248). The Dst-index dropped until -50nT and Kp-index up to 6.

Planetary indices on 1st September 2019 (G2) geomagnetic storm.



RESULTS

Case 2: Geomagnetic Storms on 31st August 2019 (G1) and 1st September 2019 (G2)



The percentage of ambiguity resolution for the GPS baselines. The dashed red box represents the day with occurrences of geomagnetic storms.

● Ambiguity Resolution:

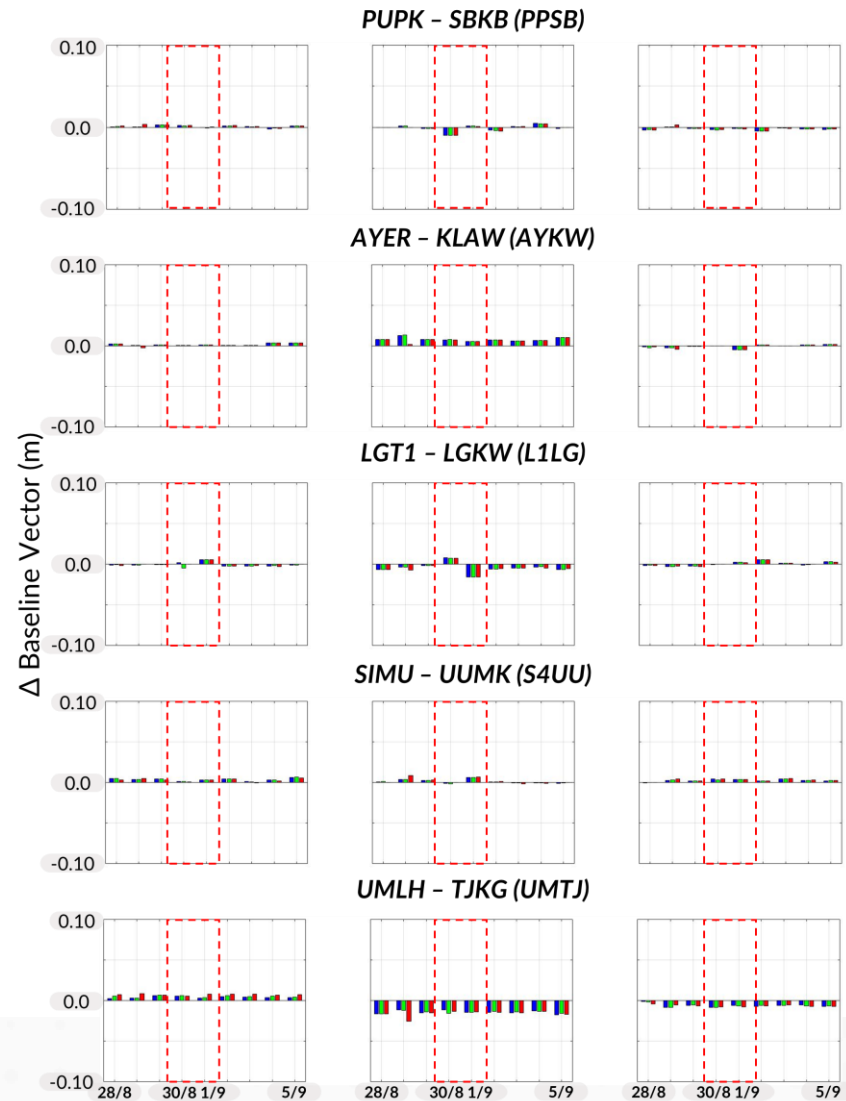
- The ambiguity resolution percentage is minimum which is expected as the occurrences of the geomagnetic storms during the study period, with a value less than 40% especially for baseline lengths less than 1000 km (during the disturbances day).

- Minimum differences between both models in improving the ambiguity resolution of the baselines, where the local ionospheric model show better improvements for short, medium, and long baseline.
- For very long baseline UMTJ, larger improvements are observed during the occurrences of the geomagnetic storms especially for global with percentage value up to 43% to 45%.
- Deterioration of the ambiguity resolution percentage was also observed with increasing baseline length – different conditions of the ionosphere (Deng et al. 2020) and due to the disturbances in ionospheric conditions as well (minimum percentage on 1st Sept compared to 31st August 2019).

RESULTS

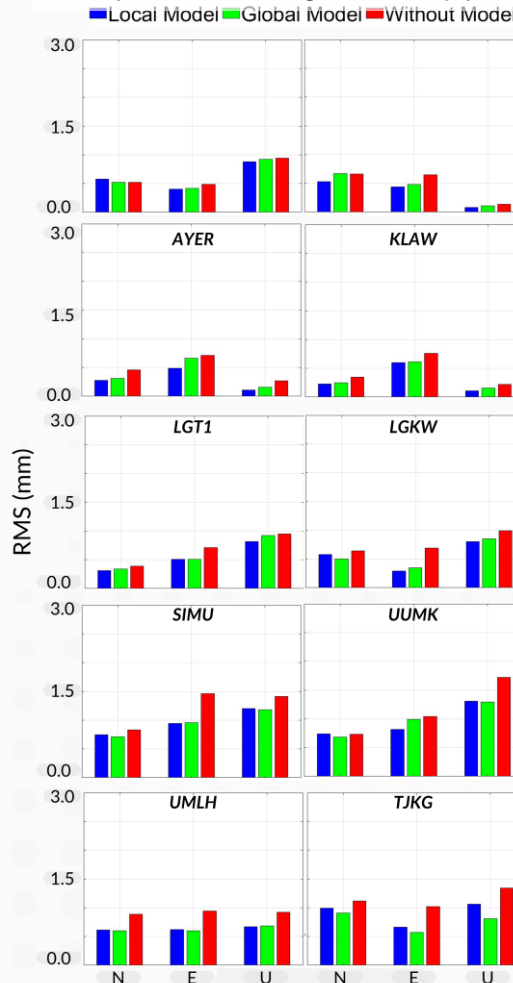
Case 2: Geomagnetic Storms on 31st August 2019 (G1) and 1st September 2019 (G2)

Local Model Global Model Without Model



Comparison of the baseline vector. The left column represents the ΔdX , the middle column represents the ΔdY and the right column represents the ΔdZ . The red boxes highlight the days with occurrences of geomagnetic storms.

RMS of station coordinates comparison during the study period.



- Comparison of Baseline Vector
 - Minimal difference in baseline vectors for both models, with values within ± 2 cm for all components.
 - The ΔdY components are found to be larger compared to other components during the study period and also for baseline UMTJ are found larger compared to other baselines.
- RMS of station coordinates
 - RMS of the stations are below 3 mm.
 - Most of the stations for baseline less than 1000 km show minimum RMS from the local ionospheric model compared to the global ionospheric model.

CONCLUSION



The results of this assessment showed that the application of the local ionospheric model served the purpose of the global ionospheric model which was able to improve the ambiguity resolution percentage, especially for baseline lengths less than 1000 km.



Although the local ionospheric model provides a low percentage of ambiguity for baseline outside the generated region, the comparison of the baseline vector still showed similar improvement as the global ionospheric model.



The performances of the global ionospheric model are undeniably suitable for application in the region (Leong et al. 2015). However, to our knowledge, there is only one station (ANMG) that is used to contribute to the development of the global ionospheric model.



Even though the local ionospheric model only shows slight differences from global ionospheric model, the results demonstrate that this can help to improve the accuracy and precision of the GPS applications, especially for near real-time applications. This assessment is also one of the initiatives for the development of the local ionospheric model over the region especially for the Malaysia region.



REFERENCES

- Assiadi M, Edwards SJ, Clarke PJ (2014) Enhancement of the accuracy of single-epoch GPS positioning for long baselines by local ionospheric modelling. *GPS Solut* 18:453-460. DOI: <https://doi.org/10.1007/s10291-013-0344-6>
- Banville S, Collins P, Zhang W, Langley RB (2014) Global and regional ionospheric corrections for faster PPP convergence. *Navigation* 61:115-124. DOI: <https://doi.org/10.1002/navi.57>
- Banville S, Langley RB, Saito S, Yoshihara T (2010) Handling cycle slips in GPS data during ionospheric plasma bubble events. *Radio Science* 45:1-14. DOI: 10.1029/2010RS004415.
- Buhari SM, Abdullah M, Hasbi AM, Otsuka Y, Yokoyama T, Nishioka M, Tsugawa T (2014) Continuous generation and two-dimensional structure of equatorial plasma bubbles observed by high-density GPS receivers in Southeast Asia. *Journal of Geophysical Research: Space Physics*. 119:10569-10580. DOI: <https://doi.org/10.1002/2014JA020433>
- Colombo OL, Hernandez-Pajares M, Juan JM, Sanz J (2002) Wide-area carrier-phase ambiguity resolution using a tomographic model of the ionosphere. *Navigation* 49:61-69. DOI: <https://doi.org/10.1002/j.2161-4296.2002.tb00255.x>
- Damaceno JG, Bolmgren K, Bruno J, Franceschi GD, Mitchell C, Cafaro M (2020) GPS loss of lock statistics over Brazil during the 24th solar cycle. *Adv Space Res* 66:219-225. DOI: <https://doi.org/10.1016/j.asr.2020.03.041>
- de Oliveira Jr PS, Monico JFG, Morel L (2020) Mitigation of receiver biases in ionospheric observables from PPP with ambiguity resolution. *Adv Space Res* 65:1941-1950. DOI: <https://doi.org/10.1016/j.asr.2020.01.037>
- Deng J, Zhang A, Zhu N, Ke F (2020) Extra wide lane ambiguity resolution and validation for a single epoch based on the triple frequency Beidou navigation satellite system. *Sensors* 20. DOI: <https://doi.org/10.3390/s20051534>
- Hernández-Pajares M, Juan JM, Sanz J, Colombo OL (2000) Application of ionospheric tomography to real-time GPS carrier-phase ambiguities resolution, at scales of 400-1000 km and with high geomagnetic activity. *Geophysical Research Letter* 27:2009-2012. DOI: <https://doi.org/10.1029/1999GL011239>
- Khamdan SS (2018) Mapping equatorial ionospheric profiles over Peninsular Malaysia using GPS Tomography. Master Thesis, Universiti Teknologi Malaysia.
- Khamdan SS, Musa TA, Buhari SM (2019) Seasonal variations of equatorial anomaly crest using GPS ionospheric tomography. *Journal of Physics: Conference Series* 1152. DOI: 10.1088/1742-6596/1152/1/012013
- Khodabandeh A, Teunissen PJG (2018) On the impact of GNSS ambiguity resolution: geometry, ionosphere, time and biases. *Journal of Geodesy* 92:637-658. DOI: <https://doi.org/10.1007/s00190-017-1084-0>
- Leong SK, Musa TA, Abdullah KA (2011) Spatial and temporal variations of GPS-Derived TEC over Malaysia from 2003 to 2009. *ISG & ISPRS* 2011:27-29.
- Leong SK, Musa TA, Omar K, Subari MD, Pathy NB, Asillam MF (2015) Assessment of ionosphere models at Banting: Performance of IRI-2007, IRI-2012 and NeQuick 2 models during the ascending phase of Solar Cycle 24. *Adv Space Res* 55:1928-1940. DOI: <https://doi.org/10.1016/j.asr.2014.01.026>
- Martiningrum DR, Yamamoto M, Pradipta R (2020) Day-to-day variability of field-aligned irregularities occurrences in nighttime F-region ionosphere over the equatorial atmosphere radar: A combinatorics analysis. American Geophysical Union, Washington. DOI:10.1002/essoar.10504367.1
- Musa TA (2007) Residual analysis of atmospheric delay in low latitude region using network-based GPS positioning. Ph.D. Thesis. Ph.D. dissertation. University of New South Wales, Australia.
- Pathy NB, Musa TA, Asillam MF, Aris WAW, Khamdan SS (2019) Near real-time ionospheric monitoring system over Malaysia using GPS Data: My-Iono Service. *Journal of Physics: Conference Series* 1152:012016. DOI: DOI 10.1088/1742-6596/1152/1/012016
- Sarudin I, Hamid NSA, Abdullah M, Buhari SM (2017) Investigation of zonal velocity of equatorial plasma bubbles (EPBs) by using GPS data. *Journal of Physics: Conference Series* 852: 012014. DOI: 10.1088/1742-6596/852/1/012014
- Silva SM, Setti Junior PT, Alves DBM, Souza EM (2020) GNSS ambiguity resolution with ration and fixed failure ratio tests for long baseline network RTK under ionospheric activity. *J Atmos Sol Terr Phys* 202. DOI: <https://doi.org/10.1016/j.jastp.2020.105256>
- Souza EM, Monico JFG (2007) GPS Ambiguity Resolution and Validation under Multipath Effects: Improvements using Wavelets. *Dynamic Planet*. 172-178. DOI: https://doi.org/10.1007/978-3-540-49350-1_27
- Sunehra D (2013) Validation of GPS receiver instrumental bias results for precise navigation. *Indian Journal of Radio & Space Physics* 42:175-181.
- Tang L, Zheng K, Li X (2017) Analysis of geometry-free residuals in case of travelling ionosphere disturbances and their impact cycle slip detection, *GPS Solut* 21:1221-1226. DOI: <https://doi.org/10.1007/s10291-017-0606-9>
- Wielgosz P, Milanowska B, Krypiak-Gregorczyk A, Jarmolowski W. (2021) Validation of GNSS-derived global ionosphere maps for different solar activity levels: case studies for years 2014 and 2018. *GPS Solut* 25:103. DOI: <https://doi.org/10.1007/s10291-021-01142-x>
- Yamakazi Y, Kosch MJ (2015) The equatorial electrojet during geomagnetic storms and substorms. *J. Geophys. Res. Space Physics* 120:2276-2287. DOI: <https://doi.org/10.1002/2014JA020773>
- Yang W, Liu Y, Liu F (2020) An Improved Ambiguity-free Method for Precise GNSS positioning with Utilizing Single Frequency Receivers. *Sensors* 20:856. DOI: <https://doi.org/10.3390/s20030856>
- Zakharenkova I, Cherniak I (2021) Effects of storm-induced equatorial plasma bubbles on GPS-based kinematic positioning at equatorial and middle latitudes during the September 7-8, 2017, geomagnetic storm. *GPS Solut* 25:132-146. DOI: <https://doi.org/10.1007/s10291-021-01166-3>
- Zhang M, Bai Z, Qian C, Fan C, Zhou P, Shu B (2017) Fast ambiguity resolution for long-range reference station networks with ionospheric model constraint method. *GPS Solut* 21:617-626. DOI: <https://doi.org/10.1007/s10291-016-0551-z>

THANK YOU

ACKNOWLEDGEMENT

Special thanks to

- Department of Survey and Mapping Malaysia – MyRTKnet data,
- Leica Geosystem ASIA, Singapore – HxGN SmartNET data (Singapore area)
- International GNSS Service (IGS) – IGS data and products
- Earth Observatory Singapore – SuGAR network data,
- Bernese GNSS software version 5.2

United Nations Office for Outer Space Affairs – Organizer for ISWI workshop 2023.



syukriahkhamdan91@gmail.com

ssyukriah2@graduate.utm.my



<https://www.linkedin.com/in/syukriahk/>

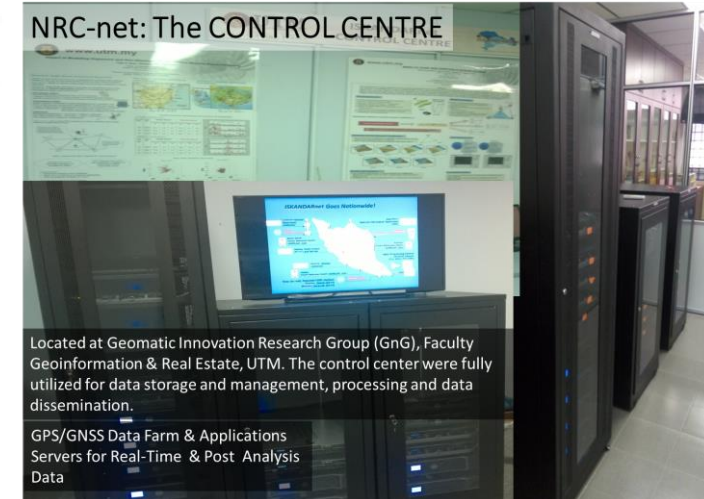
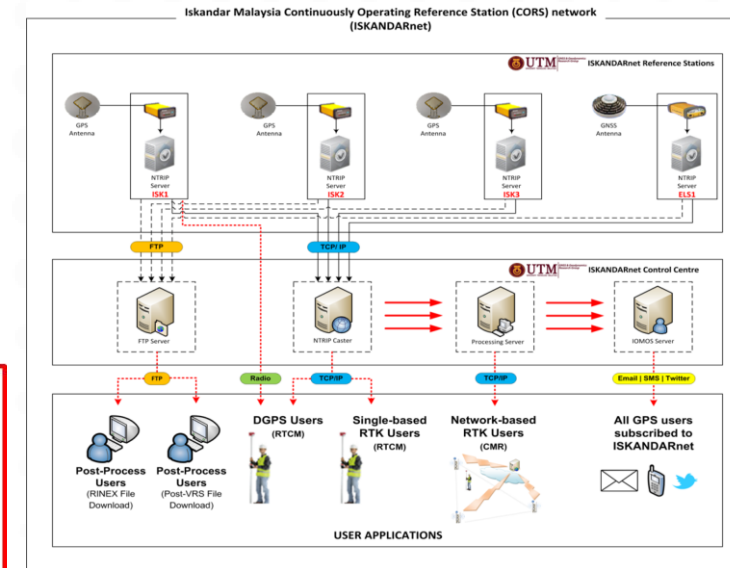
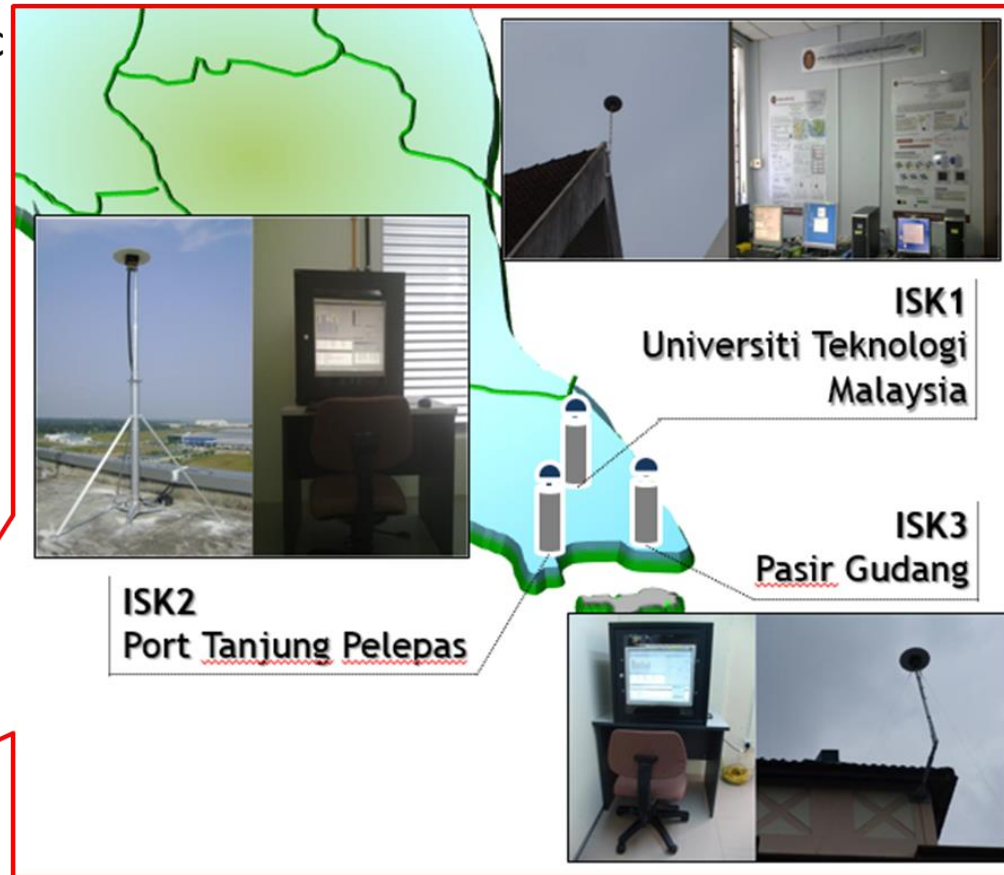
R&D INFRASTRUCTURE

ISKANDARnet - R&D CORS Network

GPS CORS network established by UTM Geomatic Innovation Research Group in the southern part of Peninsular Malaysia.



ISKANDARnet Stations



R&D Applications: Services



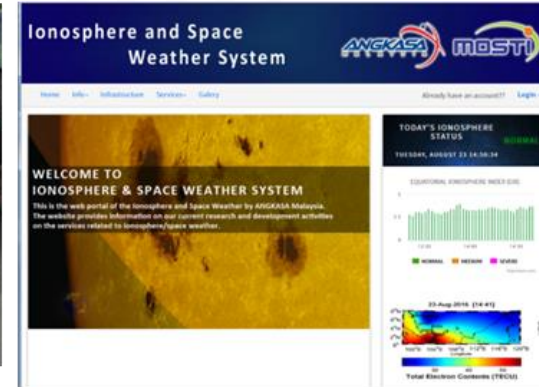
GPS/GNSS CORS network & Precise Positioning Apps



Coordinate Transformation Program



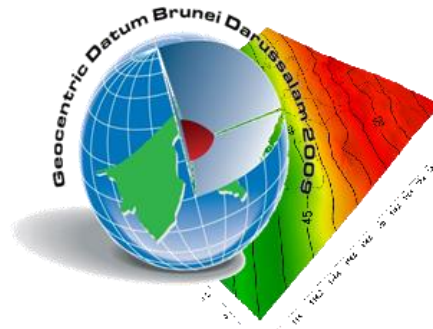
Consultancies & Courses on GPS/GNSS Data Processing & Analysis



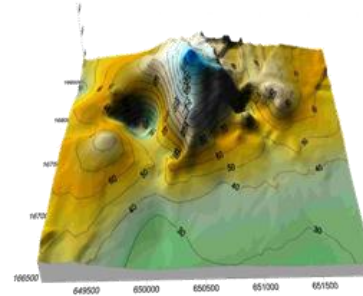
Real-time Equatorial Ionosphere index and Alert system (EIXA)



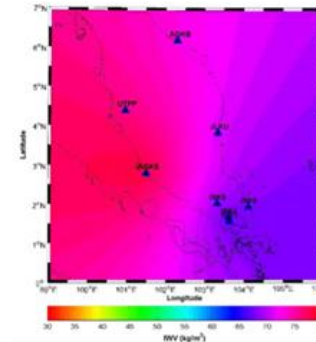
Real-time GPS/DGPS Integrity Monitoring System



Brunei Fitted Geoid & Geocentric Datum



Landslide Mapping & Monitoring Service



Near Real-Time GPS Meteorology



Positioning for Agriculture



The NRC-net infrastructure supports many research & academic activities as well as platform to develop space-based applications for the country.